Can the Nuclear Liquid Drop Model Be Improved?

Omar Yépez

E-mail: yepezoj@gmail.com

To be part of a nucleus, the constituent nucleons lose part of the original area they have. This can be measured by subtracting this area from the surface area of the nucleus. This was measured and plotted against the respective nuclear binding energy. A straight linear relationship was found for all elements, light or heavy. For a given element, the nuclear binding energy is inversely proportional to the lost original area. Thus meaning, that more area lost corresponded to a larger binding energy. β^- decay occurred to produce a nucleus with less loss of the nucleons' original area. β^+ decay occurred to produce a nucleus with less Coulomb repulsion. The nucleus stability just follows a trade-off between these two trends.

1 Introduction

Even though there is a very complete understanding of nuclear forces, they are so complicated that this knowledge can not be used to construct a complete theory of the nucleus. In other words, it is not possible to explain all nuclei properties based on the nuclear force acting between protons and neutrons. However, there is a number of models, or rudimentary theories with certain validity, which can explain a limited number of certain properties. In between those theories, the liquid drop model has been used with success and it has not changed for more than sixty years [1]. Theoretically, the nuclear liquid drop model calculates the nuclear binding energy by taking into account a number of interactions [2], i.e.

$$E_b = a_V A - a_S A^{2/3} - a_C \frac{Z(Z-1)}{A^{1/3}} - a_A \frac{(A-2Z)^2}{A} \pm \delta(A,Z) \quad (1)$$

where the coefficients a_V, a_S, a_C, a_A and $\delta(A,Z)$ are determined empirically. The volume of the nucleus is proportional to A, thus the term $a_V A$. Nucleons on the surface of the nucleus have fewer nearest neighbors. This can also be thought of as a surface tension term. If the volume term is proportional to A, the surface term should be proportional to $A^{1/3}$. The Coulomb term is due to the electric repulsion between protons in the nucleus. The asymmetry term a_A is due to the Pauli exclusion principle and the pairing term which capture the effect of spin-coupling. This formula gives the nuclear binding energy with a positive sign for exothermic reactions.

Besides its original success and continuous efforts, this model has not progressed more and still does not perform well with light nuclei [1]. There could be a number of reasons for that. Forcing a correlation between the nuclear binding energy against the number of nucleons, A; or putting several parameters to be fit against powers of A could be some of the reasons.

Nowadays, there is plenty of data about the radiuses of all isotopes for all elements, which are reported in [3]. Thus, a better correlation between the nuclear binding energy and the nucleons' surface term could be achieved. In this paper, a straight linear correlation was found between a geometrical construct that measures how much surface area has been lost by a given isotope's nucleons (Ω) and its nuclear binding energy. Changes between parent and daughter nucleus' Ω and the Coulomb repulsion are sufficient to explain β decay, emission of protons, α particles and neutrons, as well as electron capture. The nucleus stability appears as a consequence of a trade-off between these two trends.

2 Experimental

All isotope radiuses were reported in [3]. The radiuses of the proton and neutron used were: $r_p = 0.8783$ fm [3] and $r_n = 1.21$ fm [4], respectively. Assuming they are all spheres*, the formula created to compute how much of the nucleons spherical surface area has been lost or gained to form the nucleus was

$$\Omega = \frac{4\pi(r_i^2 - Zr_p^2 - Nr_n^2)}{Z+N}. \quad (2)$$

Ω is the surface area difference between the isotope and its components per number of nucleons, $A = Z + N$, in fm^2, r_i is the radius of the isotope, Z is the number of protons and N is the number of neutrons. The nuclear binding energy (mass defect) was calculated by the following formula [5]

$$E_b = (Zm_e + Zm_p + Nm_n - m_i)c^2 \quad (3)$$

where m_e, m_p and m_n are the masses of the electron, proton and the neutron respectively and m_i is the mass of the isotope. The masses of the isotopes were reported in [6], the decay mode, energy and yields were reported in [7]. The following figures present the graphs of Ω versus the nuclear binding energy for different elements. In the case of nuclear decays, $\Delta\Omega$ is the difference between daughter and parent nucleus' Ω.

3 Results

Fig. 1 shows that Ω for a given group of isotopes is inversely proportional to its nuclear binding energy. It is also observed that the rate of its change diminished as the number of protons increase. In this way, helium presents the largest changes in

*It is known the nucleus has different shapes. A sphere is one of them.

Ω within smaller changes in nuclear binding energy, whereas radon showed very small changes in Ω corresponding to larger changes in binding energy.

Fig. 2 presents Ω versus nuclear binding energy for He, Li, Be and B isotopes. The isotope with a red circle are the stable ones. It is clearly observed that as the binding energy increases, the nucleons of a given isotope presents a more negative Ω and requires more binding energy to form.

Beginning with two stable isotopes, ^{3}He's Ω is positive because the addition of the area of two protons and one neutron is not larger than the area of the isotope. Whereas ^{4}He's Ω is negative because the addition of the areas of two protons and two neutrons is larger than the area of that isotope. Once ^{6}He formed, the stability is lost. Given that ^{6}Li has a lower mass than ^{6}He, β^- decays occur, liberating 3.51 MeV. This process follows an Ω increase and therefore ΔΩ was 6.48 fm^2 for this reaction.

In the same manner, ^{8}He suffers β^- decay and neutron emission to ^{7}Li, with 16% reaction yield. It liberates 8.63 MeV. This is also accompanied by the emission of one neutron. Again, the daughter nucleus presents a more positive Ω and therefore ΔΩ = 6.41 fm^2 for this reaction.

^{8}He also suffers β^- decay to ^{8}Li, with 83% yield. It liberates 10.66 MeV and ΔΩ = 3.86 fm^2.

^{7}Be suffers 100% β^+ decay into ^{7}Li. Contrary to the previous trend, in this process the daughter presented a more negative Ω than the parent nucleus. But also, β^+ diminished the number of protons in the daughter nucleus, thus diminishing the Coulomb repulsion. Contrary to previous β^- decay, in this case ΔΩ = -3.13 fm^2.

^{9}Li repeats ^{6}He's behavior. ^{11}Li presents neutron emission to ^{10}Be with 86.3% yield and β^- decay to ^{11}Be with 6% yield*. This is very similar to ^{8}He transmutation. Finally, ^{10}Be repeats ^{6}He's behavior. Table 1 summarizes the nuclear processes observed in Fig. 2. It is clearly observed that β^- and neutron emission presents a positive ΔΩ, whereas β^+ decay shows a negative ΔΩ.

Fig. 3 presents Ω versus nuclear binding energy for O, F, Ne, Na and Mg isotopes. A 100% of ^{17}Ne transmutes to ^{16}O after β^+ decay and a proton emission, producing 11.63 MeV. ΔΩ in this case was -1.88 fm^2. A 100% of ^{19}Ne transmutes to ^{19}F after β^+ decay, producing 2.20 MeV and ΔΩ = -0.88 fm^2. ^{20}Na goes to ^{20}Ne with 75% yield, producing 12.87 MeV and ΔΩ = -0.26 fm^2. It also emits an alpha particle and a positron to produce ^{16}O with 25% yield, generating 8.14 MeV and ΔΩ = -0.26 fm^2. Table 2 presents the transitions observed in Fig. 3. It is clearly observed that β^+, proton and alpha particle emissions present a negative ΔΩ, whereas β^- and 2β^- decays show a positive ΔΩ.

Fig. 4 presents Ω versus nuclear binding energy for Ar, K, Ca, Sc and Ti isotopes. A 100% of ^{38}K transmutes to ^{38}Ar after β^+ decay, producing 4.89 MeV and ΔΩ in this case was -0.28 fm^2.

A 100% of ^{39}Ca transmutes to ^{39}K after β^+ decay, producing 6.52 MeV and ΔΩ = -0.28 fm^2. ^{40}K goes to ^{40}Ca with 89.28% yield, producing 1.31 MeV and ΔΩ = 0.30 fm^2. ^{40}K also suffers electron capture to ^{40}Ar with 10.72% yield, producing 0.48 MeV and ΔΩ = -0.24 fm^2. A 100% of ^{41}Ca transmutes to ^{41}K after β^+ decay, producing 0.42 MeV and ΔΩ = -0.32 fm^2. Also, ^{41}Ar suffers β^- decay to ^{41}Ca producing 2.49 MeV and ΔΩ = 0.21 fm^2. Table 3 depicts the transitions

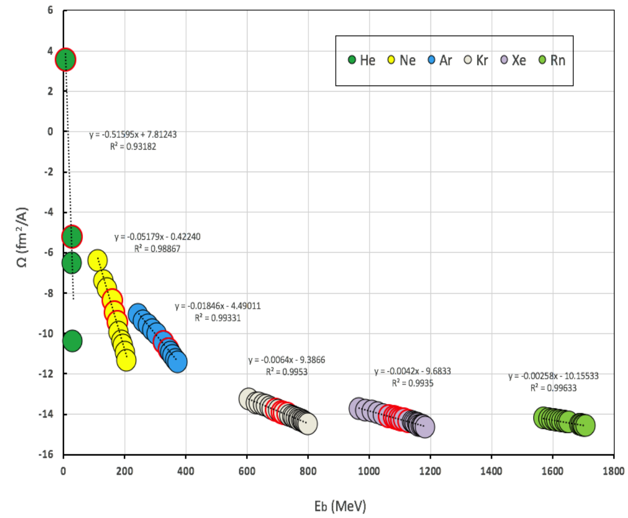

Fig. 1: Ω vs. binding energy for Noble gases. The red circles are the stable isotopes.

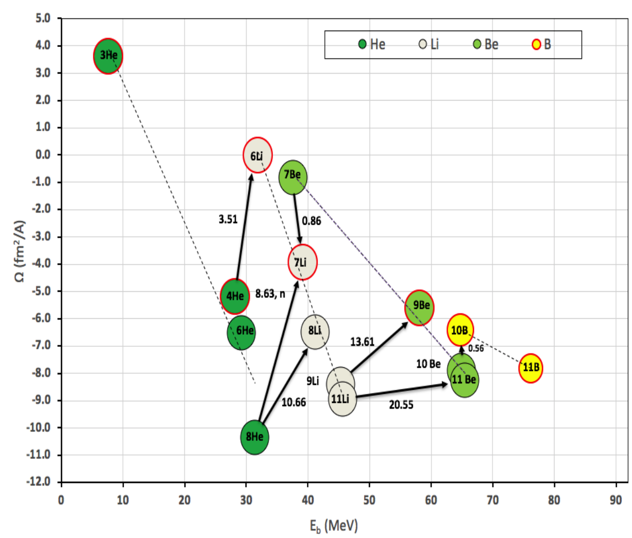

Fig. 2: Ω vs. mass defect for He, Li, Be and B isotopes. The red circles are the stable isotopes. The energy of the transitions (MeV) were reported in [7].

*This nucleus also experiences double and triple neutron emission, α emission and fission in lower yields.

Table 1: Reaction, mass and area (ΔΩ) difference between parent and daughter nuclei, and decay mode for the reactions depicted in Figure 2.

Reaction	Released Energy (MeV) [7]	ΔΩ (fm^2)	Decay
$^{4}_{2}He \rightarrow ^{6}_{3}Li + e^- + \nu$	3.51	6.48	β-
$^{8}_{2}He \rightarrow ^{7}_{3}Li + e^- + n + \nu$	8.63	6.41	β- and neutron emission
$^{8}_{2}He \rightarrow ^{8}_{3}Li + e^- + \nu$	10.66	3.86	β-
$^{7}_{4}Be \rightarrow ^{7}_{3}Li + e^+ + \nu$	0.86	-3.13	β+
$^{9}_{3}Li \rightarrow ^{9}_{4}Be + e^- + \nu$	13.61	2.79	β-
$^{11}_{3}Li \rightarrow ^{10}_{4}Be + e^- + n + \nu$	20.55	0.68	β- and neutron emission
$^{10}_{4}Be \rightarrow ^{9}_{5}B + e^+ + \nu$	0.56	1.85	β-

Table 2: Reaction, mass and area (ΔΩ) difference between parent and daughter nuclei, and decay mode for the reactions depicted in Figure 3.

Reaction	Released Energy (MeV) [7]	ΔΩ (fm^2)	Decay
$^{17}_{10}Ne \rightarrow ^{16}_{8}O + e^+ + p + \nu$	14.55	-1.88	β+ and proton emission
$^{19}_{10}Ne \rightarrow ^{19}_{9}F + e^+ + \nu$	3.24	-0.88	β+
$^{20}_{11}Na \rightarrow ^{16}_{8}O + e^+ + \alpha + \nu$	9.16	-0.26	β+ and α emission
$^{20}_{11}Na \rightarrow ^{20}_{10}Ne + e^+ + \nu$	13.89	-0.30	β+
$^{21}_{11}Na \rightarrow ^{21}_{10}Ne + e^+ + \nu$	3.55	-0.57	β+
$^{22}_{11}Na \rightarrow ^{22}_{10}Ne + e^+ + \nu$	2.84	-0.50	β+
$^{23}_{10}Ne \rightarrow ^{23}_{11}Na + e^- + \nu$	4.38	0.65	β-
$^{24}_{10}Ne \rightarrow ^{24}_{12}Mg + 2e^- + 2\nu$	7.99	1.21	2β-
$^{25}_{10}Ne \rightarrow ^{25}_{12}Mg + 2e^- + 2\nu$	11.15	0.99	2β-
$^{26}_{10}Ne \rightarrow ^{26}_{12}Mg + 2e^- + 2\nu$	16.70	0.98	2β-

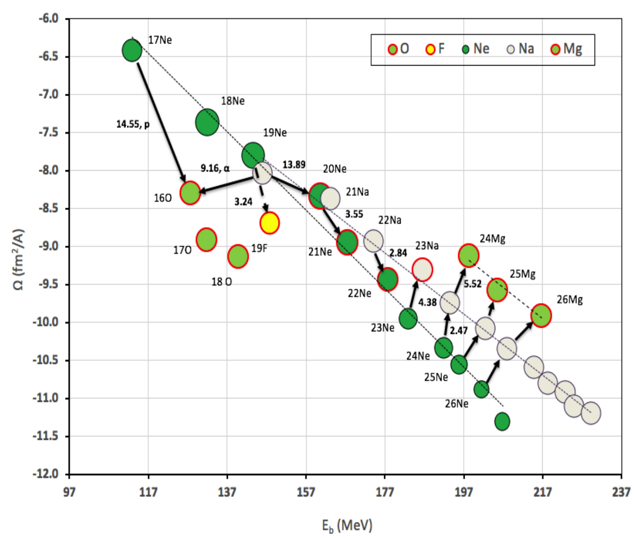

Fig. 3: Ω vs. mass defect for O, F, Ne, Na and Mg isotopes. The red circles are the stable isotopes. The energy of the transitions (MeV) were reported in [7].

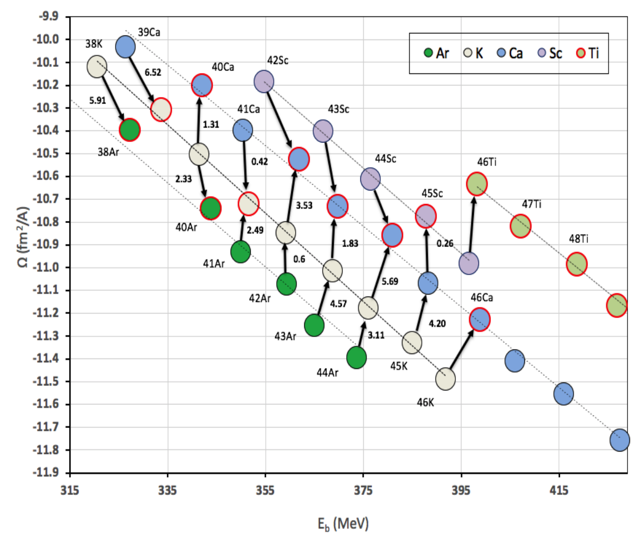

Fig. 4: Ω vs. mass defect for Ar, K, Ca, Sc and Ti isotopes. The red circles are the stable isotopes. The energy of the transitions (MeV) were reported in [7].

observed in Fig. 4. It is clearly observed that electron capture presents a negative ΔΩ.

4 Discussion

4.1 Meaning of Ω and the Nuclear Liquid Drop Model

Ω was computed by using one dimension (the radius) and the three dimensions (the volume). All elements kept a good linear relationship between Ω and the nuclear binding energy. However, in the case of helium, either the linear relationship was lost or the isotopes did not occur proportionally. For example: ^{6}He occurred between ^{3}He and ^{4}He. This relationship is also very sensitive to the neutron radius. Overall, to keep ^{4}He to land between ^{3}He and ^{6}He, r_n needs to be at least 0.05 fm larger than r_p. This may be an indication that the spherical model is only partly applicable to helium. According to the results presented in Fig. 1, it seems that a surface-based Ω is a fundamental property of the isotopes of any element. Given the nature of Ω, it is obvious that larger changes per nucleon would occur in the lowest mass element, helium. This is because the number of nucleons is the lowest. As the number of protons increase, Ω changes less because it is divided by a progressively larger number of nucleons. In a given element, Ω becomes more negative because the addition of the area of the components of the nucleus is progressively larger than its isotope's area. This corresponds to an increasing nuclear binging energy. Which can be interpreted as more energy is

Table 3: Reaction, mass and area (ΔΩ) difference between parent and daughter nuclei, and decay mode for the reactions depicted in Figure 4.

Reaction	Released Energy (MeV) [7]	ΔΩ (fm^2)	Decay
${}^{38}_{19}\mathrm{K} \rightarrow {}^{38}_{18}\mathrm{Ar} + e^{+} + \nu$	5.91	-0.28	β^+
${}^{39}_{20}\mathrm{Ca} \rightarrow {}^{39}_{19}\mathrm{K} + e^{+} + \nu$	6.52	-0.28	β^+
${}^{40}_{19}\mathrm{K} \rightarrow {}^{40}_{18}\mathrm{Ca} + e^{-} + \nu$	1.31	0.30	β^-
${}^{40}_{19}\mathrm{K} \rightarrow {}^{40}_{18}\mathrm{Ar} + e^{+} + \nu$	1.50	-0.24	EC
${}^{41}_{20}\mathrm{Ca} \rightarrow {}^{41}_{19}\mathrm{K} + e^{+} + \nu$	0.41	-0.32	β^+
${}^{41}_{18}\mathrm{Ar} \rightarrow {}^{41}_{19}\mathrm{K} + e^{-} + \nu$	2.49	0.21	β^-
${}^{42}_{18}\mathrm{Ar} \rightarrow {}^{42}_{20}\mathrm{Ca} + 2e^{-} + 2\nu$	4.10	0.55	$2\beta^-$
${}^{43}_{18}\mathrm{Ar} \rightarrow {}^{43}_{20}\mathrm{Ca} + 2e^{-} + 2\nu$	6.40	0.53	$2\beta^-$
${}^{44}_{18}\mathrm{Ar} \rightarrow {}^{44}_{20}\mathrm{Ca} + 2e^{-} + 2\nu$	9.07	0.54	$2\beta^-$
${}^{45}_{19}\mathrm{K} \rightarrow {}^{45}_{21}\mathrm{Sc} + 2e^{-} + 2\nu$	4.46	0.55	$2\beta^-$

needed to compress the nucleons' area into the nucleus. This means that all nucleons share the nucleus surface.

This proportionality between the nuclear binding energy and the surface lost to create the nucleus contrasts with the semi-empirical mass formula (1). This is because Fig. 1 presents explicitly that the nuclear binding energy is just proportional to the normalized nucleons' surface area lost to form the isotope. As will be discussed, the other important term is the Coulomb repulsion. This makes (1) to have too many terms to fit. This is because the underlying model for (1) is a sphere-like structure with the neutrons and protons gathered together but still separated as individual spherical particles. The underlying model that Fig. 1 suggests is one where all nucleons share the surface of the nucleus. Which means that protons and neutrons are blended, fused.

4.2 Calculation of ^{8}Be's radius

Not shown in Fig. 2, ^{8}Li transmutes to ^{8}Be and this decays into two ^{4}He. ^{8}Be is not shown in Fig. 2 because its radius was not reported in [3]. An estimation of ^{8}Be's radius can be accomplished by using the inverse proportion between Ω and the other Be isotopes. Fig. 5 shows the result. ^{8}Be nuclear binding energy is 56.50 MeV. Thus, its Ω = -5.65 fm^2 and the calculated ^{8}Be radius was 2.31 fm. This puts ^{8}Be and ^{9}Be at the same Ω as shown in Fig. 5.

4.3 Why a decay occurs

Fig. 2 depicts the helium isotopes in more detail. Given that ^{2}He is unstable, it seems that helium needs at least one neutron for stability, which occurs in ^{3}He. This suggests the neutron is acting as a Coulomb repulsion insulator. This effect continues in ^{4}He. However, ^{5}He and heavier isotopes become unstable again. It seems that there is a limit to how much area can be lost from the nucleons to form the nucleus, after which a decay is needed to resolve the instability. The first beta decay occurs between the more massive parent ^{6}He and

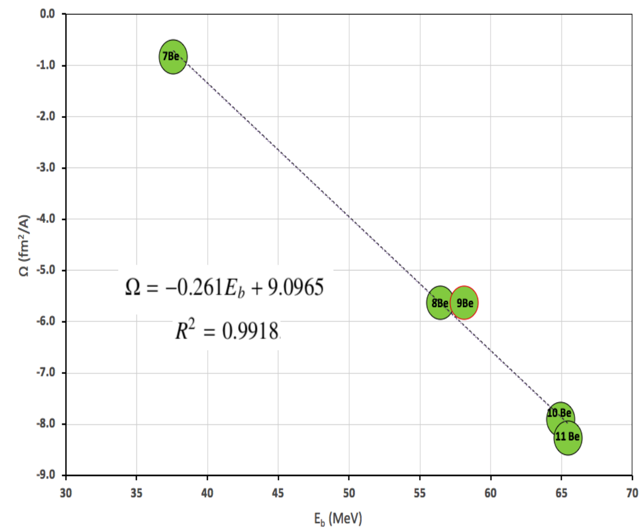

Fig. 5: Ω vs. mass defect for B isotopes. The red circle is the stable isotope.

the lighter daughter ^{6}Li producing 3.51 MeV. As observed, β^- decay involves: *to go from a heavier and lower Coulomb repulsion, which has more nucleons' surface area lost (NSL), to a lighter and higher Coulomb repulsion, which has less NSL.* Therefore, the driving force for β^- decay is to reduce the NSL. This is why the ΔΩ for this reaction is positive. This is a feature of β^- decay and several examples where ΔΩ is positive are shown in Tables 1, 2 and 3. In a more complicated process with 16% reaction yield , ^{8}He suffered neutron emission and β^- decay to transmute to ^{7}Li. This process, nevertheless, has the same features already described for β^- decay, i.e. in neutron emission ΔΩ is also positive. Another example of a positive Ω is ^{11}Li going to ^{10}Be.

^{7}Be is the first example of β^+ decay to ^{7}Li. As observed, this process involves: *to go from a heavier and higher Coulomb repulsion nucleus, which has less NSL, to a lighter and lower Coulomb repulsion nucleus, which has more NSL.* This is why the ΔΩ for this reaction is negative. Hence, the driving force for β^+ decay is to reduce the Coulomb repulsion. Other examples can be observed in Tables 2 and 3.

Fig. 3 shows that: a) ^{17}Ne transmutes to ^{16}O with 100% yield suffering β^+ decay and proton emission and b) ^{20}Na transforms into ^{16}O by the emission of an α particle and a positron. In both cases, ΔΩ is negative. Therefore, these processes are driven by the reduction of Coulomb repulsion.

Fig. 4 presents ^{40}K suffering β^-decay to ^{40}Ca with 89.28% yield. This overwhelms the β^+ decay to ^{40}Ar with 10.72% yield. This reaction suggests that, in this case, to reduce the nucleons' surface area lost is more favorable than to reduce its Coulomb repulsion.

4.4 Nucleus stability

It seems that there is a trade-off between the NSL and Coulomb repulsion for nucleus stability. In Fig. 2, ^{3}He increases the NSL until it reaches ^{6}He. Then, β decay increases the number of protons to produce ^{6}Li. But also to reduce the original NSL in ^{6}He.

At the same Coulomb repulsion,^{6}Li increases the NSL until it reaches ^{9}Li. Again, β decay diminished the NSL transmuting to ^{9}Be. This element starts again to increase NSL up to ^{10}Be, which again β decayed to ^{10}B to diminish NSL and so on. Hence, every time the surface area per nucleon increases to the unstable limit, β decay occurs to resolve the instability. This produces continuous step decreases all through stable nuclei. The process just described pass through different elements. For example, in Fig. 3 there is an increase in the NSL in the series ^{16}O:^{17}O:^{18}O. Then, there is a small NSL decrease through continuous elements, creating the row ^{18}O:^{19}F:^{20}Ne. This is occurring even though the Coulomb repulsion is increasing. The NSL increases in Ne again, following the series ^{20}Ne:^{21}Ne:^{22}Ne.

Then, another small NSL decrease occurs through elements, forming the row ^{22}Ne:^{23}Na:^{24}Mg with progressive increments in Coulomb repulsion. This is followed by another increase in the NSL in the series ^{24}Mg:^{25}Mg:^{26}Mg. In Fig. 4, the first small decrease in NSL is observed in the row ^{38}Ar:^{39}K:^{40}Ca. If we follow this row, the next element would be ^{41}Sc. This isotope is unstable because it has too much Coulomb repulsion for the small NSL decrease trade-off. As a consequence, the next stable nucleus occurs in an increase of the NSL, producing ^{40}Ar, which also is accompanied by a significant decrease in Coulomb repulsion. From ^{40}Ar a new row of small decrease of the NSL but progressive increase in Coulomb repulsion starts again, ^{40}Ar:^{41}K:^{42}Ca. This will end at ^{43}Sc, which is unstable for the same reasons discussed above.

Once ^{42}Ca is reached, a new trend of increasing NSL started, ^{42}Ca:^{43}Ca:^{44}Ca. This makes a hole in stability for ^{41}Ca. This isotope is not stable because ^{41}K presented a more favorable trade-off between the NSL and Coulomb repulsion. The next row would be ^{44}Ca:^{45}Sc:^{46}Ti. And the next series ^{46}Ti: ^{47}Ti:^{48}Ti and so on.

^{46}Ca however, appeared as an outlier in this trend. It could be argue that it makes a row with ^{46}Sc but it does not decay to it. It looks like it is an island of NSL stability.

The evidence presented calls to build a model where all nucleons share the surface of the nucleus.

5 Conclusions

The nuclear binding energy is directly related to the nucleons' surface area lost (NSL). A trade-off between the NSL and the Coulomb repulsion is related to the nucleus stability. The progressive increase of the mass in an element will produce different isotopes until its NSL reaches an upper limit for its Coulomb repulsion. Then, β^{-} decay or neutron emission occur to diminish the NSL and resolve the instability. If there is not enough neutrons (electric insulation) for a given Coulomb repulsion, β^{+} decay, proton or α emission occur to diminish it.

Received on March 7, 2020

References

1. Pomorski K. and Dudek J. P. Nuclear Liquid Drop Model with the Surface-Curvature Terms: New Perspectives for the Hyperdeformation Studies. arXiv: nucl-th/0205011.
2. Möller P. The limits of the nuclear chart set by fission and alpha decay. *EPJ Web of Conferences*, 2016, v. 131, 03002.
3. Angeli I. and Marinova K. P. Table of experimental nuclear ground state charge radii: An update. *Atomic Data and Nuclear Data Tables*, 2013, v. 99, 69.
4. Abrahamyan S. et al. (PREX Collaboration). Measurement of the Neutron Radius of ^{208}Pb through Parity Violation in Electron Scattering. *Phys. Rev. Lett.*, 2012, v. 108, 112502.
5. Pourshahian S. *J. Am. Soc. for Mass Spec.*, 2017, v. 28, 1836.
6. Wang M., Audi G., Kondev F. G., Huang W. J., Naimi S. and Xu X. The AME2016 atomic mass evaluation (II). Tables, graphs, and references. *Chinese Physics C.*, 2017, v. 41 3, 030003.
7. Audi G., Kondev F. G., Wang M., Huang W. J. and Naimi S. The NUBASE2016 evaluation of nuclear properties. *Chinese Physics C.*, 2017, v. 41 3, 030001.